Rock Mechanics and Rock Engineering
https://doi.org/10.1007/s00603-021-02574-0

ORIGINAL PAPER

The Effect of Pre-heating Treatment and Water–Cement Ratio on the Shearing Behavior and Permeability of Granite–Cement Interface Samples

Fan Zhang[1] · Tanzhuo Cheng[1] · Zhenzhen Zhu[1] · Dawei Hu[2] · Jianfu Shao[1,3]

Received: 14 August 2020 / Accepted: 6 July 2021

Abstract
The shearing behavior and permeability of the interfaces between rock and cement are critical for the stability analysis of supporting structures in underground engineering projects, especially after exposure to thermal loads. In the present study, an advanced test method was proposed to preform shearing tests on granite–cement interface samples after pre-heating treatment. The samples consisted of two semi-cylindrical parts. The first part was granite, and the other was cement with two different water–cement ratios (for example, 0.3 and 0.5). The shear stress–strain curves, peak shear strength at shear failure, as well as the residual shear strength at the residual shear stage, cohesion, and internal shear angle, were analyzed. The results were correlated to the pre-heating temperatures and cement–water ratios, while the initial permeability before shear loading, along with the permeability evolution during the shearing process, was also analyzed. It was found that after higher pre-heating treatment the lower the peak shear strength, cohesion, and internal friction angle of the samples would be. Meanwhile, the initial permeability was higher. In addition, during the shearing process, the shear stress and permeability levels increased rapidly, reaching maximum values when shear failure occurred. Then, the shear stress and permeability levels decreased gradually to stable values at the residual shear stage. The degradation in the shear strength, cohesion, and internal friction angle caused by the pre-heating treatment may be attributed to the microcracks induced by the thermal expansion differences between the granite and cement and the evaporation of the chemically bound water in the cement. The shearing behavior and permeability evolution of the granite–cement interface samples were determined to be closely related to the water–cement ratios. For example, under the same normal stress and pre-heating temperature conditions, when the water–cement ratio was higher, the porosity of the cement was greater and the adhesion between the granite–cement interfaces was lower. Therefore, the peak shear strength at the shear failure point was also lower. In addition, the shear stress–strain curves showed stronger ductile behavior, and the cohesion and internal friction angle were lower. Meanwhile, the reductions in the shear stress and permeability levels at the residual shear stage became smaller.

Keywords Granite–cement interfaces · Shearing behavior · Permeability · Pre-heating treatment · Water–cement ratios

1 Introduction

Rock-cement interfaces are widely used in many underground engineering projects, such as tunnels, and underground geological repositories for nuclear waste storage. The shearing and permeability behavior of the interfaces between rock and cement are critical for the stability analyses of underground engineering projects. Under the conditions of occasional fire accidents during transportation processes in tunnels, or heat generated from High-level Radioactive Waste (HLW) in HLW repositories, the shearing behavior of rock-cement interfaces could potentially be significantly changed. Such changes could consequently

✉ Jianfu Shao
jian-fu.shao@polytech-lille.fr

[1] School of Civil Engineering, Architecture and Environment, Hubei University of Technology, Wuhan, China

[2] State Key Laboratory of Geomechanics and Geotechnical Engineering, Institute of Rock and Soil Mechanics, Chinese Academy of Sciences, Wuhan, China

[3] Univ. Lille, CNRS, Centrale Lille, UMR 9013 - LaMcube - Laboratoire de Mécanique, Multiphysique, Multi-échelle, 59000 Lille, France

Published online: 20 July 2021

result in additional shearing deformations and permeability variations at the rock-cement interfaces (Ebeling et al. 2000; Andjelkovic et al. 2015). Therefore, the shearing behavior and permeability of the rock-cement interfaces are considered to be of major importance to the safety assessments of underground engineering projects (Fox and Ross 2011; Kwak et al. 2013).

A great number of studies have reported important findings regarding the experimental characterization of the mechanical properties of rock-cement interfaces. In recent years, indirect test methods have been developed to calibrate the mechanical properties of the aforementioned interfaces (Aquino et al. 1995; Mindess 1996; Tasong et al. 1999; Bentur and Alexander 2000; Caliskan 2003; Rao and Prasad 2004; Wang et al. 2012). It has been found that there are many factors which may potentially affect the shear strength levels of the interfaces. The main factors include the mixture ratios of the concrete; roughness and scales of the interfaces; and external static and dynamic loads (Hutchinson and Suo 1992; Fishman and Pal 1994; Lee and Buyukozturk 1995; Buyukozturk and Hearing 1998; Bergado et al. 2006; Agrawal and Karlsson 2007; Buzzi et al. 2008; Yang et al. 2008; Chen et al. 2010; Fall and Nasir 2010; Zhong et al. 2014; Luo et al. 2017).

Moreover, due to the fact that underground structures may be exposed to occasional fire accidents or heating process from HLW, the effects of heating treatment on the mechanical properties of granite and cement have also been extensively studied (Mambou et al. 2015; Borinaga-Treviño et al. 2018; Zhang et al. 2018a, b, c; Krishna et al. 2019; Yang et al. 2019a, b; Bai et al. 2020). It has been determined that when the heating temperature is below 400 °C, the physical and mechanical properties of granite basically remain unchanged (Chen et al. 2017). Some slight attenuating effects may be observed in the temperature range of 400 to 600 °C (Liu and Xu 2014). Then, when the temperature levels exceed 600 °C, the heating-induced attenuating effects tend to be more pronounced (Yang et al. 2017). However, it has also been found that relatively low heating temperature may lead to deterioration of the cement. In the present study, it was observed that as the temperature levels rose above room temperature, the free water in the samples gradually evaporated. Then, when the temperature exceeded 105 °C, the bound water also began to evaporate. It was found that when the temperature continued to rise and exceeded 400 °C, the calcium hydroxide contained in the cement mortar began to decompose. During the aforementioned process, the pore structures inside the mortar changed, which affected the physical properties of the mortar (Neville 1995; Zhang et al. 2017, 2018a, b, c).

However, to the best of the author's knowledge, there remains a lack of investigation results regarding the influencing effects of pre-heating treatment on the shearing behavior and permeability levels of granite–cement interfaces. Therefore, to address this issue, an advanced shearing and permeability test method was adopted in this study to perform laboratory tests on granite–cement interface samples after pre-heating treatment. Different values of pre-heating temperature (150 and 250 °C) and water–cement ratios (0.3 and 0.5) were considered in this study's experiments. The shear stress–strain curves, permeability variations, and the peak shear strength at the shear failure point were examined, as well as the residual shear strength at the residual shear stage, cohesion, and internal shear angles. In addition, the effects of the different pre-heating treatment and water–cement ratios on the shearing behavior and permeability levels of the granite–cement interface samples were discussed in detail.

2 Sample Preparation and Experimental Testing Scheme

2.1 Preparation Method for the Granite–Cement Interface Samples

The samples which were examined in this study were cylindrical and consisted of two semi- cylindrical parts. One part was composed of granite, and the other was poured cement (Fig. 1). The granite used in this study was collected from Tuanshan Village located in China's Hunan Province. The petro-physical analysis results using an X-ray diffraction technique (Bruker D8 Advance X-ray diffractometer) showed that the mineral composition of the granite was mainly composed of feldspar, pyroxene, and quartz in the following percentages: potassium feldspar (46.16%), feldspar (35.02%), pyroxene (12.14%), and quartz (6.68%). The density was 2.62 g/cm^3, and the average porosity was 0.07%. In addition, ordinary Portland cement (PO32.5) and standard sand (ISOR 679-68) were used to prepare the cement parts of the samples. From the viewpoint of the practical applications, two water–cement ratios (w/c) were selected. The mixture mass ratios of the poured cement are detailed in Table 1.

Fig. 1 Images of the granite–cement interface samples

Table 1 Mixture ratios of the cement mortar by weight

Cement	Sand	Water
1	2.45	0.5
1	2	0.3

For the cement with water–cement ratios (*w*/*c*) of 0.3, 2 g of a polycarboxylic acid water-reducing agent were added per 202.5 g of water. It was observed that with the appropriate use of a water-reducing agent, the workability and strength of the mixture could be significantly improved. For example, when the cement particles were evenly dispersed, the wrapped water could be easily released with the addition of a water-reducing agent. Subsequently, the amount of the water could be reduced to achieve the requirements of the cement flow. Under those conditions, the dry density and water retention of the cement stabilized aggregates were effectively improved (Hu et al. 2018). In the present research investigation, after the cement was poured into the other half of the samples, sealed containers with constant temperatures of 25 °C and 100% relative humidity were used to cure the granite–cement interface samples. The samples remained in the curing room for approximately 520 days after the set-up of experimental device. The long curing time was implemented to avoid the effects of curing time on the shearing behavior of the granite–cement interface samples. It was considered that relatively small changes in the mechanical properties of the cement would be generated after the first 3 months (Neville 1995).

In addition, the shear strength levels of the interfaces are known to be dependent on the roughness values. In other words, with increases in the roughness values of the samples, the shear strength levels of the interfaces increased (Shen et al. 2019). In addition, considering that tunnel boring machines are widely used for the rock excavations in practical applications, and the degrees of roughness of excavation surfaces tend to be relatively lower, a mechanical cutting method was used in this study to produce the semi-cylindrical parts of the granite samples used in this study's experimental tests. The roughness degrees of the granite interfaces were measured using a 3D non-contact profilometer was 5.51 μm. Since the textures of the granite interfaces were observed to be uniform, the roughness variations could be ignored were not taken into consideration in this study. Three samples were prepared for each test condition. The average values were used for the analysis of the obtained results.

2.2 Pre-heating Treatment

Prior to the implementation of this study's shearing tests, the granite–cement interface samples were heated in a furnace at atmospheric pressure, with a heating rate of 1 °C/min until a prescribed temperature was reached. This low pre-heating rate was used to keep the thermal gradient as small as possible, and to ensure that the cracking processes were merely induced by the temperature effects and not by the thermal gradients throughout the samples. Two levels of pre-heating temperatures (150 °C and 250 °C) were selected. After a stabilization period of five hours at the pre-heating temperature, the samples were cooled to room temperature in a furnace at ambient pressure at a rate of 1 °C/min. Finally, all of the samples were placed into a desiccator at 105 °C until the subsequent tests were completed.

2.3 Steps for the Shearing and Permeability Tests

This study's shearing and permeability tests were conducted using a self-designed autonomous testing system, as shown in Fig. 2a. Three servo hydraulic pumps were used to apply normal stress, shear stress, and pore pressure to the interfaces, respectively. The maximum shear force was 1000 kN, and the maximum normal stress and pore pressure were both 60 MPa. The shear strain was measured using two transducers (LVDTs) which were placed between the bottom and top platens inside the confining cell. In addition, to ensure the accuracy of the test results, the average value of the two transducers was used to eliminate any installation errors.

In the present study, an advanced shear and permeability test method (Fig. 2b) was developed for the purpose of conducting shearing and permeability tests on granite–cement interface samples. A special shear disc was designed to allow the generation of shearing deformations and fluid transport along the interfaces (Liu et al. 2020; Ding et al. 2020), as detailed in Fig. 2c. The designed shear disc was 50 mm in diameter and had a thickness of 10 mm, and consisted of two different materials (rigid steel and silica gel) with different stiffness values. The two shear discs were placed opposite each other on the upper and lower surfaces of the samples for the purpose of converting the axial force into shear stress along the interfaces. Moreover, some seepage channels were prefabricated to allow water transport along the interfaces during the shearing processes.

The experimental shearing and permeability tests were performed under room temperature conditions of 25 °C. The detailed testing procedure was as follows:

(1) Shearing tests: The normal stress σ was applied to the target value and then maintained as a constant. The initial permeability of the samples was first measured under a constant normal stress of 5 MPa and a steady head of 2 MPa. Then, shear stress was applied to the interfaces of the granite–cement at a loading rate of 0.01 mm/min until the end of the shearing tests. The shear stress–strain curves of the samples were recorded by a data acquisition system.

Fresh et al. (2019a, b) calibrated the shear stress obtained from the triaxial direct-shear condition on

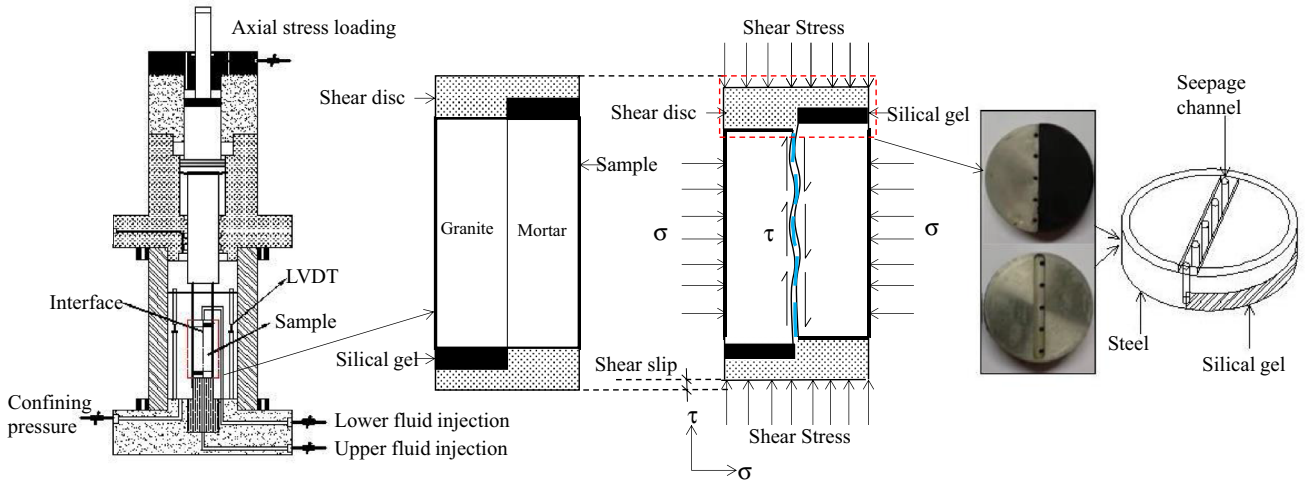

(a) Autonomous testing system **(b) Shearing and permeability test methods** **(c) Shearing disc**

Fig. 2 Diagram of the experimental testing equipment

two Teflon semi-cylindrical samples using the shear test method adopted in this study. Liu et al. (2020) and Ding et al. (2020) also performed shearing tests on the interfaces of concrete and claystone and cracked granite using the same shearing test method. The previous results indicated that the additional resistance caused from the deformed silicone could be ignored and the axial force applied on the samples could be considered as identical to the shear force. Therefore, the shear stress in this study's testing processes was calculated using the following:

$$\tau = \frac{F}{A}, \tag{1}$$

where τ is the shear stress of the granite–cement interface (MPa); F represents the shearing force of the granite–cement interface (N); and A indicates the interface area of the granite–cement sample (mm^2), which is identical to the product of the diameter and length of the sample.

Although the roughness degrees of the interfaces were relatively low, the cementation between the rock and cement is considered to be of major importance for the analysis of the shearing behavior (Liu et al. 2020). Therefore, it was assumed in this study that the shear strength levels of granite–cement interfaces could be described by the linear Mohr–Coulomb failure criterion as follows:

$$\tau = c + \sigma \tan \varphi, \tag{2}$$

where c and φ are the cohesion (MPa) and internal friction angle (°) of the interface, respectively.

(2) Permeability tests: The permeability levels of the samples were measured using a steady head method at different times during the shearing processes. Distilled water was used as the fluid flow medium, and a constant pressure difference of 2 MPa was applied at the inlets of the samples. The flow rates at the outlets were measured every hour, and the permeability experiments were considered to be completed when the flow rates at the outlets achieved a stable state. The permeability levels of the samples were calculated using Darcy's Law as follows:

$$Q = kS\frac{\Delta p}{\mu L}, \tag{3}$$

where Q is the flow rate (m^3/s) of the samples; k indicates the permeability (m^2) of the samples; μ represents the viscosity (Pa.s) of the transport fluid; Δp is the pore pressure difference (Pa) between the input and output; and S and L denote the cross-sectional area (m^2) and the length (m) of the samples, respectively.

3 Test Results

As mentioned above, shearing and permeability tests under three different normal stress conditions were performed on granite–cement interface samples with two different water–cement ratios following heating treatment. The steps of the experimental testing processes are listed in Table 2.

Table 2 Scheme of the shearing and permeability experimental tests

Water–cement ratio	Pre-heating temperature (°C)	Normal stress (MPa)
0.5, 0.3	25 (unheated), 150, 250	5, 10, 15

To account for any experimental scattering, three tests were conducted for each group of samples, and the average values were then calculated from the three tests.

3.1 Shearing Behavior

The typical shear stress–strain curves of the granite–cement interface samples following the heating treatment are presented in Fig. 3. As can be seen in the figure, for the different examined normal stress, the shear stress–strain curves of the samples with both water–cement ratios showed similar trends under different pre-heating temperature conditions. The shear stress first increased up to the peak shear strength level at the point of shear failure, which was followed by decreases in the residual shear strength level at the residual shear stage. To analyze the effects of the different pre-heating treatment on the shearing behavior, the variations in peak shear strength of the granite–cement interface samples after different pre-heating temperatures were applied are plotted in Fig. 4. It was found that the peak shear stress was continuously decreased with the increasing of the pre-heating temperatures for the samples under the three different normal stress conditions and the two different water–cement ratios. This study selected the water–cement ratio of 0.5 and the normal stress of 5 MPa as examples. The shear strength of the unheated sample was 9.02 MPa. Then, following the heating treatment, the shear strength was determined to have decreased to 7.48 MPa at the pre-heating temperature of 150 °C, and to 6.23 MPa at the pre-heating temperature of 250 °C. These results indicated that the pre-heating treatment had clear degradation effects on the shear strength levels of the examined granite–cement interface samples.

Moreover, at the same levels of normal stress and pre-heating temperatures, the shear stress–strain curves of the granite–cement interface samples with a water–cement ratio of 0.5 (Fig. 3a, c, e) showed more important ductile behavior than those with a water–cement ratio of 0.3 (Fig. 3b, d, f). Furthermore, the peak shear strength levels at the point of shear failure of the former group were lower than that of the latter group. It was determined by taking the examples of the sample under the conditions of a normal stress of 15 MPa and a pre-heating temperature of 25 °C that the peak shear strength and residual shear strength at the residual shear stage (as well as their differences) were 17.30, 16.84, and 0.46 MPa for water–cement ratio of 0.5, respectively. Meanwhile, the peak shear strength and residual shear strength (as well as their differences) were 20.16, 15.80, and 4.36 MPa for the samples with a water–cement ratio of 0.3. Therefore, it was concluded that the water–cement ratios also had significant effects on the shearing behavior of the granite–cement interface samples in this study.

The relationships between the peak shear strength levels and the normal stress of the samples after different pre-heating temperatures are detailed in Fig. 5. It can be seen in the figure that the corresponding peak shear strength envelopes were successfully obtained. Using Eq. (2), the values of the cohesion and internal friction angle were calculated, as detailed in Table 3. It should be noted that three parallel tests were performed for each condition and the average value was used for this study's analyses. Figure 6 shows the evolutions of the cohesion and frictional angles with the different pre-heating temperatures. It can be seen in the figure that with the increases in the pre-heating temperatures, the cohesion and internal friction angle continually decreased for the samples with both water–cement ratios. However, the deceasing rate in the cohesion of the samples with a water–cement ratio of 0.3 was slightly smaller than those with a water–cement ratio of 0.5.

3.2 Permeability Variations

The effects of the different pre-heating treatment on the initial permeability of the samples before shear stress loading were first analyzed. The variations in the initial permeability levels with the increasing of the pre-heating temperatures are shown in Fig. 7. It was observed that the initial permeability levels increased gradually with the increasing of the pre-heating temperatures, and those increases in the initial permeability levels were determined to be closely related to the pre-heating induced microcracks. Moreover, under the same pre-heating temperature conditions, the initial permeability levels were lower when the normal stress was higher. This phenomenon indicated that the pre-heating induced microcracks were closed to some extent under the loading of the normal stress.

The results of previous related studies have indicated that the permeability of granite is relatively low (less than 10^{-18} m^2) for heating temperatures ranging between 25 and 300 °C (Zhang et al. 2018a, b, c; Cao 2018; Yang et al. 2019a, b). In the present investigation, the permeability of the cement alone after the heating treatment was measured and the maximum value was determined to be 2.26×10^{-18} m^2 (Table 4). Therefore, considering that the permeability levels of the granite or cement alone were significantly less than that of the granite–cement interface samples, the granite–cement interface zones were considered to contribute the majority of the fluid transport pathways of the samples.

The permeability evolution of the granite–cement interface samples during the shearing processes are detailed in Figs. 8, 9, 10. It can be seen in the figures that the permeability-shear strain curves of the samples were similar to the shear stress–strain curves for all the normal stress and pre-heating temperature conditions. More precisely, the permeability levels were found to increase rapidly to the maximum values at the point of shear failure. Then, with continuous increases in the shearing displacements after shear failure,

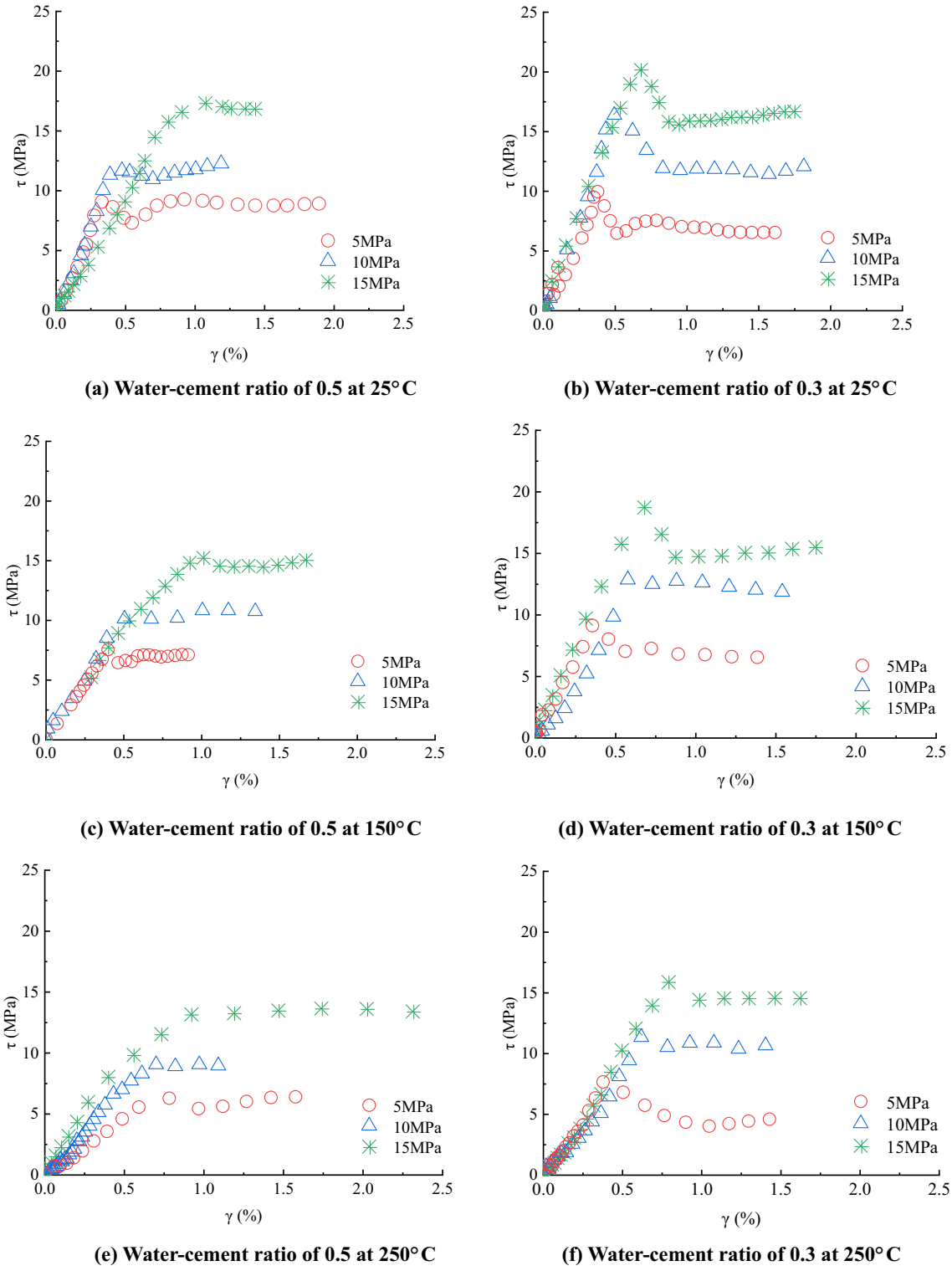

Fig. 3 Typical shear stress–strain curves of the granite–cement interface samples

the permeability levels were observed to gradually decrease to stable values at the residual shear stage. The increases in permeability were attributed to the occurrences of the crack openings related to the shear dilation mechanism prior to shear failure. Meanwhile, the decreases in permeability were attributed to the appearances of the crack closures related to the asperity shear-off mechanism after shear failure occurred. In addition, the drops in the permeability

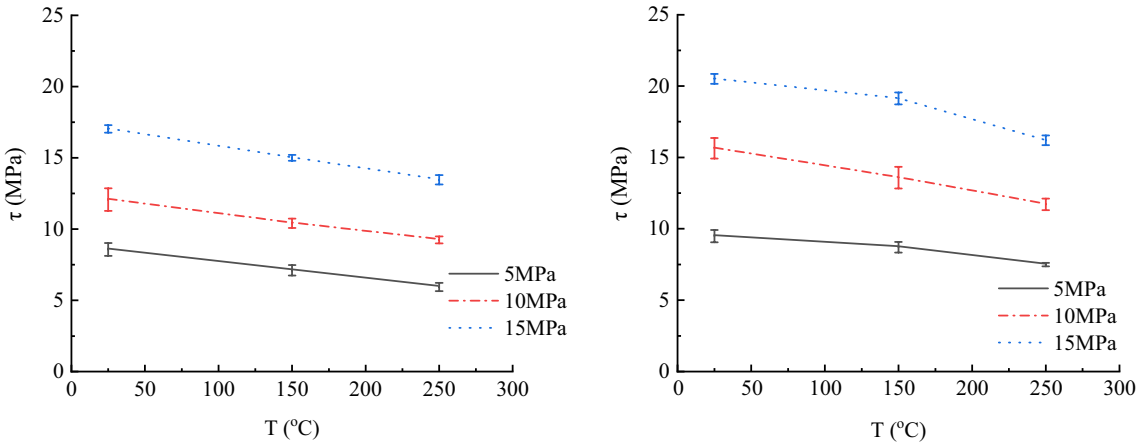

Fig. 4 Relationships between the shear strength levels and the pre-treatment temperature levels

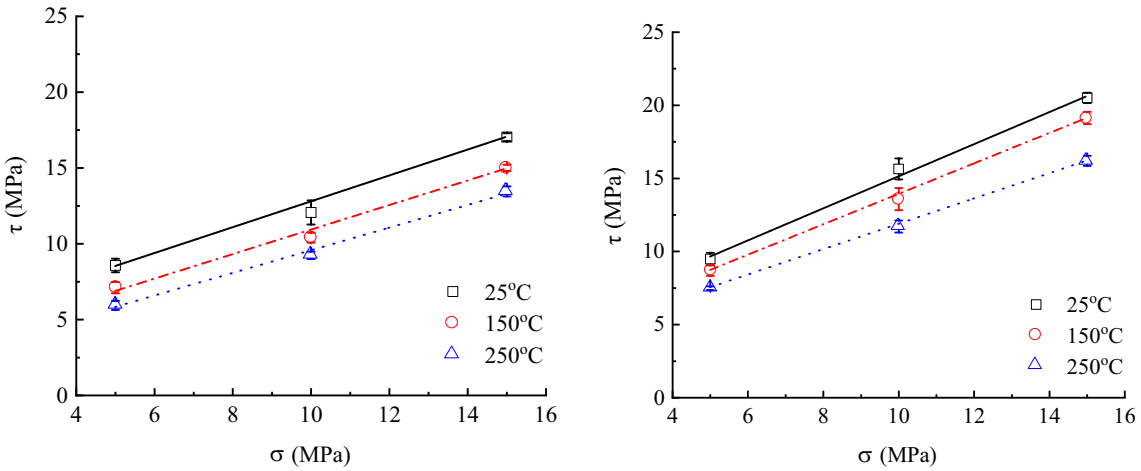

Fig. 5 Shear envelopes for the different pre-heating temperatures

Table 3 Cohesion and internal friction angle for the different pre-heating temperatures

Temperature (°C)	Cohesive stress (MPa)		Internal friction angle (°)	
	w/c = 0.5	*w/c* = 0.3	*w/c* = 0.5	*w/c* = 0.3
25	4.09	4.19	40.25	49.7
150	2.95	3.38	38.29	48.3
250	2.03	3.10	36.90	42.5

levels of the samples with water–cement ratios of 0.3 were determined to be greater than those of the samples with water–cement ratios of 0.5, under the same pre-heating temperature and normal stress conditions.

4 Discussion

The results of this study showed that the pre-heating treatment had significant effects on the shearing behavior and initial permeability of the examined granite–cement interface samples. The degradations in the peak shear strength, cohesion, and internal friction angle may be attributed to the following two mechanisms: (1) Microcracks were induced due to different thermal expansion coefficients between the granite and the cement; (2) Chemical changes occurred due to evaporation of the chemically bound water. Previous related studies have shown that the thermal expansion coefficients of cement are approximately 1.7 times that of granite after pre-heating treatment at 250 °C

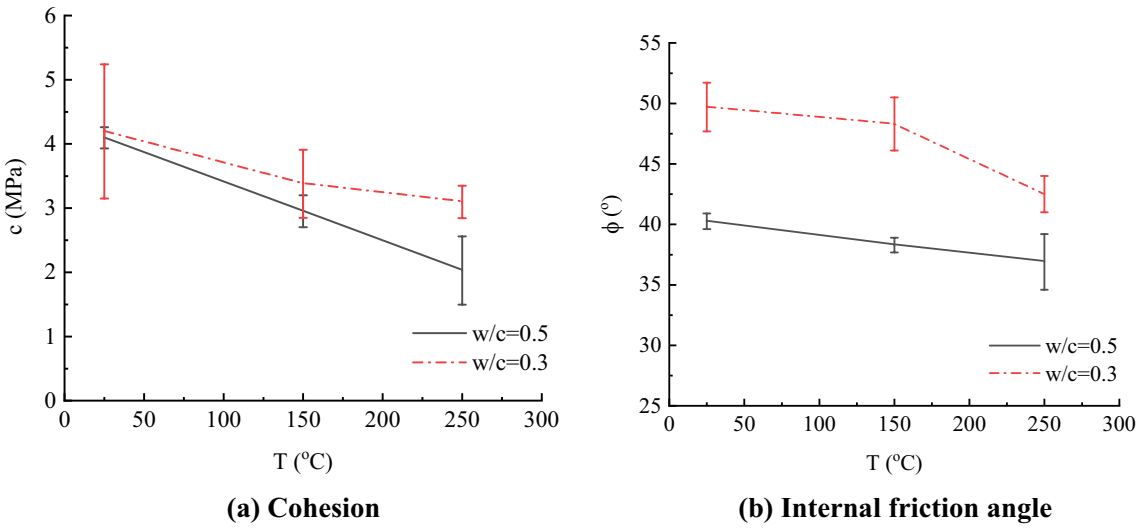

Fig. 6 Evolution of the cohesion and internal frictional angle with the different pre-heating temperatures

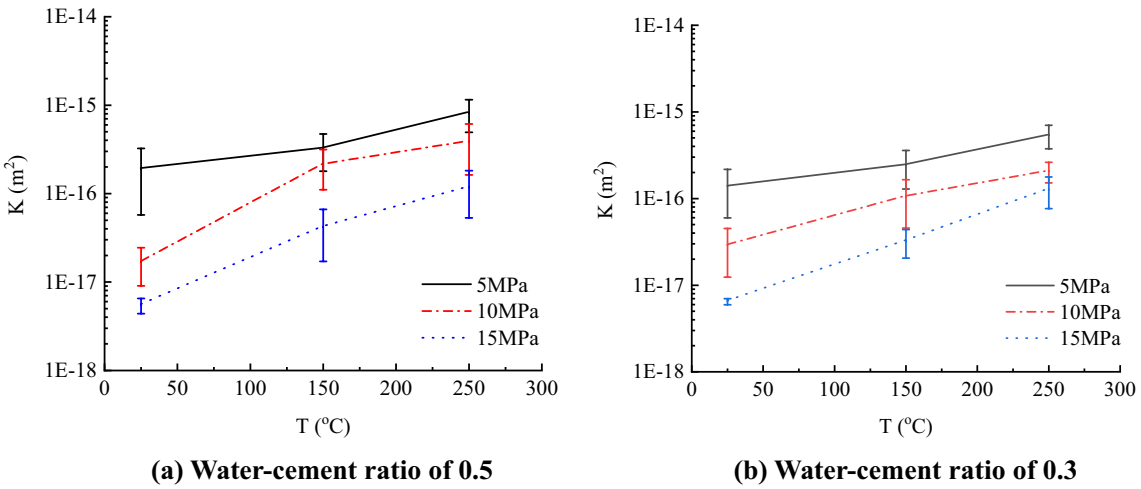

Fig. 7 Evolution of the initial permeability levels of the granite–cement interfaces with the different pre-treatment temperatures

Table 4 Permeability of the cement alone after different values of pre-treatment temperatures

Normal stress (MPa)	Permeability of cement mortar (m^2)					
	25 °C		150 °C		250 °C	
	w/c = 0.5	*w/c* = 0.3	*w/c* = 0.5	*w/c* = 0.3	*w/c* = 0.5	*w/c* = 0.3
5	4.12×10^{-20}	1.01×10^{-21}	1.16×10^{-18}	1.67×10^{-20}	2.26×10^{-18}	2.67×10^{-19}
10	–	–	3.53×10^{-19}	1.04×10^{-20}	5.84×10^{-19}	1.41×10^{-19}
15	–	–	1.85×10^{-19}	4.58×10^{-21}	5.06×10^{-19}	9.81×10^{-20}

(Wan et al. 2008). In addition, the different thermal expansion coefficients between the granite and the cement could potentially lead to the generation of new microcracks in the interface zones (Lion et al. 2005; Ramos et al. 2016; Sabih et al. 2018). Moreover, the chemically bound water will evaporate at temperature ranges between 100 and 300 °C (Zhang et al. 2018a, b, c), and these variations in moisture content may cause the interfacial transition zones

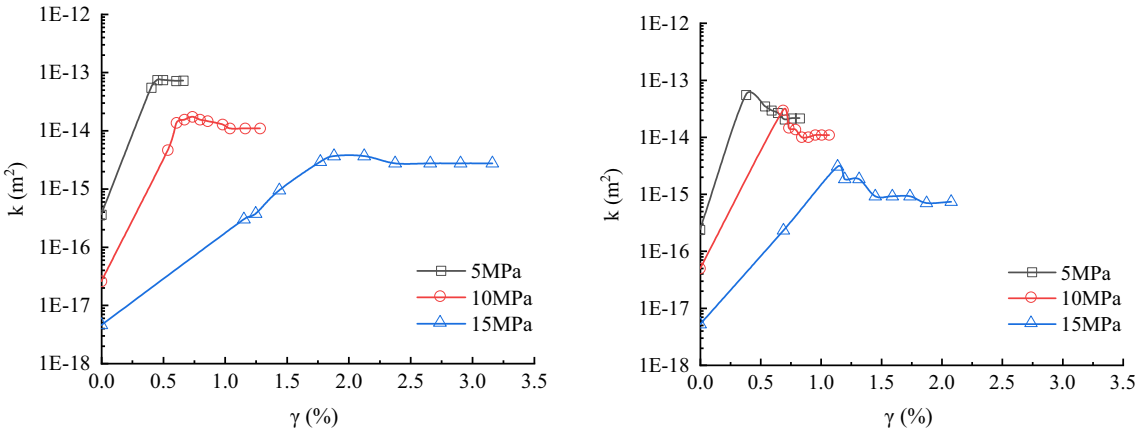

(a) Water-cement ratio of 0.5 **(b) Water-cement ratio of 0.3**

Fig. 8 Relationships between the permeability levels and the shear strain values under different normal stress conditions at a room temperature of 25 °C

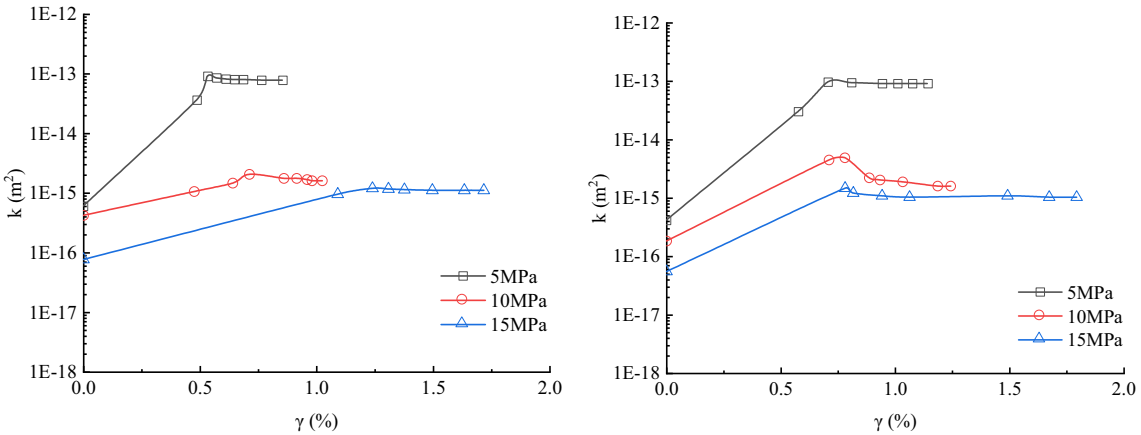

(a) Water-cement ratio of 0.5 **(b) Water-cement ratio of 0.3**

Fig. 9 Relationships between the permeability levels and shear strain values under different normal stress conditions after 150 °C thermal treatment

between the cement paste and the coarse aggregates to weaken (Ichikawa and England 2004; Malik et al. 2020). The aforementioned pre-heating induced microcracks and the chemical changes would then reduce the mechanical properties and offer fluid transport pathways, consequently causing the degradation of the shearing strength and increases in the initial permeability.

It was established in this study that the shearing behavior and permeability evolution of the granite–cement interface samples were closely related to the water–cement ratios. For example, under the same normal stress and pre-heating temperature conditions, when the water–cement ratio was high (for example, 0.5), the peak shear strength level at shear failure tended to be lower. Meanwhile, the shear stress–strain curves displayed important ductile behavior, and the cohesion and internal friction angle were also lower. Subsequently, the drops in the shear stress and permeability values at the residual shear stage were smaller. The water–cement ratios also determined the porosity and volume of the voids of the hardened cement paste at all of the hydration stages. For example, when the water–cement ratios were higher than about 0.38, the volume of the gel was not sufficient to fill all the space available. Therefore, some of the volume of the capillary pores was left even after the process of hydration had been completed (Neville 1995). Therefore, for the granite–cement interface samples with higher water–cement ratios, the porosity of cement was greater and the adhesion of the granite–cement interfaces was smaller (Chen et al. 2016), which resulted in lower shear strength values and greater deformation ability, with decreased reductions in the

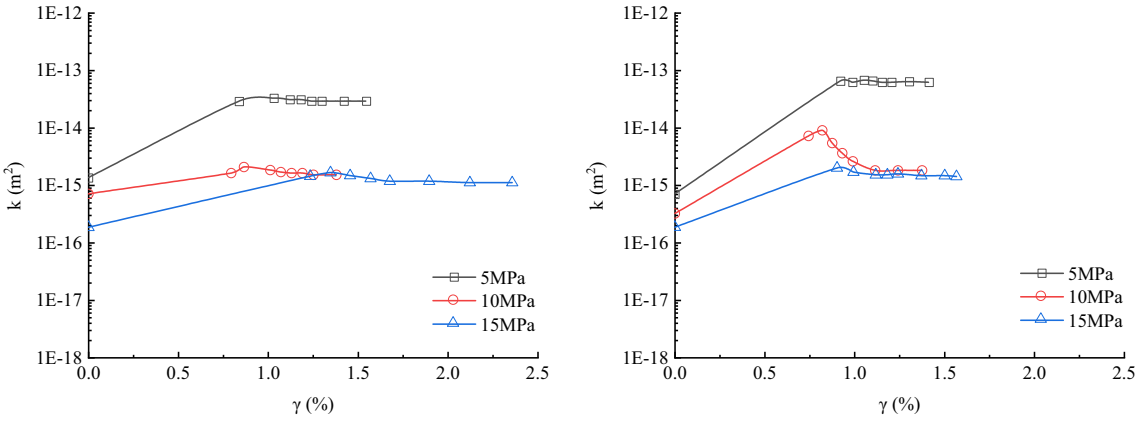

(a) Water-cement ratio of 0.5 **(b) Water-cement ratio of 0.3**

Fig. 10 Relationships between the permeability levels of the samples and the shear strain under different normal stress conditions after 250 °C thermal treatment

shear stress levels after shear failure occurred (Saiang et al. 2005; Eskandari-Naddaf and Kazemi 2018). Similar results have been also observed in related research regarding other types of rock-cement interfaces (Atahan et al. 2009; Tracz 2016; Li et al. 2020).

5 Conclusions

This study conducted experimental shearing and permeability tests on granite–cement interface samples after pre-heating treatment using an advanced testing method. The effects of different pre-heating temperatures and water–cement ratios on the shear strength, cohesion, internal friction angle, and permeability levels were analyzed. It was found that the pre-heating temperatures had significant effects on the shearing behavior and initial permeability levels of the samples prior to the shear stress loading. This study found that under the same normal stress and water–cement ratio conditions, when the pre-heating temperatures were higher, the peak shear strength at the point of shear failure, as well as the cohesion and internal friction angle, were lower. These degradation effects on the peak shear strength, cohesion, and internal friction angle may be attributed to the induced microcracks, since the thermal expansion coefficients between the granite and the cement were different. Also, chemical changes occurred due to the evaporation of the chemically bound water. The pre-heating induced microcracks and the chemical changes reduced the mechanical properties and provided fluid transport pathways which consequently caused the degradation of the shearing behavior and increases in the initial permeability levels. Furthermore, when comparing the two different water–cement ratios, this study found that the peak shear strength at shear failure was lower and the shear stress–strain curves showed stronger ductile behavior, and the drops in the shear stress and permeability values at the residual shear stage were smaller for the samples with higher water–cement ratios. The granite–cement interface samples with higher water–cement ratio were characterized with greater porosity in the cement portions, causing the adhesion of the granite–cement interfaces to be smaller. This resulted in lower shear strength, greater deformation ability, and lower drops in the shear stress values after shear failure. In the present study, considering that the studied values of the water–cement ratios were very limited, other water–cement ratio values will be taken into account in subsequent research investigation.

Acknowledgements This research was jointly supported by the National Key Research and Development Program of China (Nos. 2018YFC0809600, 2018YFC0809601), and the Natural Science Foundation of China (Grant numbers 51979100, 51779252, and 51579093).

References

Agrawal A, Karlsson AM (2007) On the reference length and mode mixity for a bimaterial interface. J Eng Mater Technol 129(4):580–587

Andjelkovic V, Pavlovic N, Lazarevic Z, Nedovic V (2015) Modelling of shear characteristics at the concrete–rock mass interface. Int J Rock Mech Min Sci 76:222–236. https://doi.org/10.1016/j.ijrmms.2015.03.024

Aquino MJ, Li Z, Shah SP (1995) Mechanical properties of the aggregate and cement interface. Adv Cem Based Mater 2(6):211–223. https://doi.org/10.1016/1065-7355(95)90040-3

Atahan HN, Oktar ON, Tademir MA (2009) Effects of water–cement ratio and curing time on the critical pore width of hardened cement paste. Constr Build Mater 23(3):1196–1200. https://doi.org/10.1016/j.conbuidmat.2008.08.011

Bai Y, Wang Y, Xi Y (2020) Modeling the effect of temperature gradient on moisture and ionic transport in concrete. Cement

Concr Compos 106:103454. https://doi.org/10.1016/j.cemconcomp.2019.103454
Bentur A, Alexander MG (2000) A review of the work of the RILEM TC 159-ETC: engineering of the interfacial transition zone in cementitious composites. Mater Struct 33(2):82–87
Bergado DT, Ramana GV, Sia HI, Varun. (2006) Evaluation of interface shear strength of composite liner system and stability analysis for a landfill lining system in Thailand. Geotext Geomembr 24(6):371–393. https://doi.org/10.1016/j.geotexmem.2006.04.001
Borinaga-Treviño R, Orbe A, Norambuena-Contreras J, Canales J (2018) Effect of microwave heating damage on the electrical, thermal and mechanical properties of fibre-reinforced cement mortars. Constr Build Mater 186:31–41. https://doi.org/10.1016/j.conbuildmat.2018.07.108
Buyukozturk O, Hearing B (1998) Crack propagation in concrete composites influenced by interface fracture parameters. Int J Solids Struct 35(35):4055–4066. https://doi.org/10.1016/S0020-7683(97)00300-4
Buzzi O, Boulon M, Deleruyelle F, Besnus F (2008) Hydromechanical behaviour of rock-Bentonite interfaces under compression. Rock Mech Rock Eng 41(2):343–371
Caliskan S (2003) Aggregate/mortar interface: influence of silica fume at the micro-and macro-level. Cement Concr Compos 25(4–5):557–564. https://doi.org/10.1016/S0958-9465(02)00095-1
Cao C (2018) Numerical interpretation of transient permeability test in tight rock. J Rock Mech Geotech Eng 10(1):32–41. https://doi.org/10.1016/j.jrmge.2017.07.009
Chen YM, Lin WA, Zhan TL (2010) Investigation of mechanisms of bentonite extrusion from GCL and related effects on the shear strength of GCL/GM interfaces. Geotext Geomembr 28(1):63–71. https://doi.org/10.1016/j.geotexmem.2009.09.006
Chen X, Lu YB, Teng X, Su S (2016) Experimental study on split tension of mortar-aggregate interface transition zone. China Concr Cement Prod 4:10–16 (**in Chinese**)
Chen YL, Wang SR, Ni J, Azzam R, Fernandez-Steeger TM (2017) An experimental study of the mechanical properties of granite after high temperature exposure based on mineral characteristics. Eng Geol 220:234–242. https://doi.org/10.1016/j.enggeo.2017.02.010
Ding CD, Zhang Y, Teng Q, Hu DW, Zhou H, Shao JF, Zhang CQ (2020) A method to experimentally investigate injection-induced activation of fractures. J Rock Mech Geotech Eng 12(6):1326–1332. https://doi.org/10.1016/j.jrmge.2020.04.002
Ebeling RM, Foster L, Jones HW, Taylor R, Bumworth J (2000) Evaluation and comparison of stability analysis and uplift criteria for concrete gravity dams by three federal agencies (No. ERDC/ITL-TR-00-1). Army Engineer Waterways Experiment Station Vicksburg Ms Engineer Research and Development Center
Eskandari-Naddaf H, Kazemi R (2018) Experimental evaluation of the effect of mix design ratios on compressive strength of cement mortars containing cement strength class 42.5 and 52.5 MPa. Proc Manuf 22:392–398. https://doi.org/10.1016/j.promfg.2018.03.060
Fall M, Nasir O (2010) Mechanical behaviour of the interface between cemented tailings backfill and retaining structures under shear loads. Geotech Geol Eng 28(6):779–790
Fishman KL, Pal S (1994) Further study of geomembrane/cohesive soil interface shear behavior. Geotext Geomembr 13(9):571–590. https://doi.org/10.1016/0266-1144(94)90011-6
Fox PJ, Ross JD (2011) Relationship between NP GCL Internal and HDPE GMX/NP GCL interface shear strengths. J Geotech Geoenviron Eng ASCE 137(8):743–753
Frash LP, Carey JW, Welch NJ (2019a) EGS collab experiment 1 geomechanical and hydrological properties by triaxial direct shear. In: 44th workshop on geothermal reservoir engineering. Stanford University.
Frash LP, Carey JW, Welch NJ (2019b) Scalable en echelon shear-fracture aperture-roughness mechanism: theory, validation, and implications. J Geophys Res Solid Earth 124(1):957–977
Hu L, Liu Z, Sha A (2018) Water reducing agent effects on the engineering performance of cement stabilized aggregates. Sci Iran Trans A Civil Eng 25(5):2404–2412
Hutchinson JW, Suo ZG (1992) Mixed mode cracking in layered materials. Adv Appl Mech 29(08):63–191
Ichikawa Y, England GL (2004) Prediction of moisture migration and pore pressure build-up in concrete at high temperatures. Nucl Eng Des 228(1–3):245–259. https://doi.org/10.1016/j.nucengdes.2003.06.011
Krishna DA, Priyadarsini RS, Narayanan S (2019) Effect of elevated temperatures on the mechanical properties of concrete. Proc Struct Integr 14:384–394. https://doi.org/10.1016/j.prostr.2019.05.047
Kwak CW, Park IJ, Park JB (2013) Evaluation of disturbance function for geosynthetic–soil interface considering chemical reactions based on cyclic direct shear tests. Soils Found 53(5):720–734. https://doi.org/10.1016/j.sandf.2013.08.010
Lee KM, Buyukozturk O (1995) Fracture toughness of mortar-aggregate interface in high-strength concrete. Mater J 92(6):634–642
Li ZP, Zhang LZ, Chu YT et al (2020) Research on influence of water-cement ratio on reinforcement effect for permeation grouting in sand layer. Adv Mater Sci Eng. https://doi.org/10.1155/2020/5329627
Lion M, Skoczylas F, Ledésert B (2005) Effects of heating on the hydraulic and poroelastic properties of Bourgogne limestone. Int J Rock Mech Min Sci 42(4):508–520. https://doi.org/10.1016/j.ijrmms.2005.01.005
Liu S, Xu J (2014) Mechanical properties of Qinling biotite granite after high temperature treatment. Int J Rock Mech Min Sci 100(71):188–193. https://doi.org/10.1016/j.ijrmms.2014.07.008
Liu Z, Shao J, Zha W, Xie S, Bourbon X, Camps G (2020) Shear strength of interface between high-performance concrete and claystone in the context of a French radioactive waste repository project. Géotechnique. https://doi.org/10.1680/jgeot.19.P.098
Luo L, Li X, Tao M, Dong L (2017) Mechanical behavior of rock-shotcrete interface under static and dynamic tensile loads. Tunn Undergr Space Technol 65:215–224. https://doi.org/10.1016/j.tust.2017.03.005
Malik M, Bhattacharyya SK, Barai SV (2020) Thermal and mechanical properties of concrete and its constituents at elevated temperatures: a review. Constr Build Mater. https://doi.org/10.1016/j.conbuildmat.2020.121398
Mambou LLN, Ndop J, Ndjaka JMB (2015) Modeling and numerical analysis of granite rock specimen under mechanical loading and fire. J Rock Mech Geotech Eng 7(1):101–108. https://doi.org/10.1016/j.jrmge.2014.07.007
Mindess S (1996) Tests to determine the mechanical properties of the interfacial zone. RILEM report, pp 47–63
Neville AM (1995) Properties of concrete. Longman, London
Ramos V, Fernandes I, Silva AS, Soares D, Fournier B, Leal S, Noronha F (2016) Assessment of the potential reactivity of granitic rocks—petrography and expansion tests. Cem Concr Res 86:63–77. https://doi.org/10.1016/j.cemconres.2016.05.001
Rao GA, Prasad BR (2004) Influence of type of aggregate and surface roughness on the interface fracture properties. Mater Struct 37(5):328–334
Sabih G, Rahman T, Tarefder RA (2018) Quantifying the impact of coefficient of thermal expansion of overlay concrete on unbonded concrete overlay performance. Heliyon 4(10):e00855. https://doi.org/10.1016/j.heliyon.2018.e00855
Saiang D, Malmgren L, Nordlund E (2005) Laboratory tests on shotcrete-rock joints in direct shear, tension and compression. Rock Mech Rock Eng 38(4):275–297

Shen Y, Wang Y, Yang Y, Sun Q, Luo T, Zhang H (2019) Influence of surface roughness and hydrophilicity on bonding strength of concrete-rock interface. Constr Build Mater 213:156–166. https://doi.org/10.1016/j.conbuildmat.2019.04.078

Tasong WA, Lynsdale CJ, Cripps JC (1999) Aggregate-cement paste interface: Part I. Influence of aggregate geochemistry. Cement Concr Res 29(7):1019–1025. https://doi.org/10.1016/S0008-8846(99)00086-1

Tracz (2016) Open porosity of cement pastes and their gas permeability. Bull Pol Acad Sci Tech Sci 64(4):775–783

Wan Z, Zhao Y, Dong F, Feng Z, Zhang N, Wu J (2008) Experimental study on mechanical characteristics of granite under high temperatures and triaxial stresses. Chin J Rock Mechan Eng 27(1):72–77 (**in Chinese**)

Wang Y, Wu SX, Shen DJ, Zhou JK (2012) Experimental study of dynamic axial tensile mechanical properties of mortar-granite interface. Rock Soil Mech 33(5):1326–1332 (**in Chinese**)

Yang S, Song LI, Li ZHE, Huang S (2008) Experimental investigation on fracture toughness of interface crack for rock/concrete. Int J Mod Phys B 22:6141–6148

Yang SQ, Ranjith PG, Jing HW, Tian WL, Ju Y (2017) An experimental investigation on thermal damage and failure mechanical behavior of granite after exposure to different high temperature treatments. Geothermics 65:180–197. https://doi.org/10.1016/j.geothermics.2016.09.008

Yang D, Wang W, Chen W, Tan X, Wang L (2019a) Revisiting the methods for gas permeability measurement in tight porous medium. J Rock Mech Geotech Eng 11(2):263–276. https://doi.org/10.1016/j.jrmge.2018.08.012

Yang J, Fu LY, Zhang W, Wang Z (2019b) Mechanical property and thermal damage factor of limestone at high temperature. Int J Rock Mech Min Sci 117:11–19. https://doi.org/10.1016/j.ijrmms.2019.03.012

Zhang X, Yang J, Deng D (2017) Research on compressive strength of recycled cement mortar after high temperature. In: IOP conference series: materials science and engineering, vol 167, No. 1. IOP Publishing, Bristol, pp 012055.

Zhang DM, Yang YS, Yang H, Chu YP, Yang S (2018a) Experimental study on the effect of high temperature on the mechanical properties and acoustic emission characteristics of gritstone. Results Phys 9:1609–1617. https://doi.org/10.1016/j.rinp.2018.05.013

Zhang F, Zhao J, Hu D, Shao J, Sheng Q (2018b) Evolution of bulk compressibility and permeability of granite due to thermal cracking. Géotechnique 69:1–11

Zhang Y, Sun Q, Yang X (2018c) Changes in color and thermal properties of fly ash cement mortar after heat treatment. Constr Build Mater 165:72–81. https://doi.org/10.1016/j.conbuildmat.2018.01.029

Zhong H, Ooi ET, Song C, Ding T, Lin G, Li H (2014) Experimental and numerical study of the dependency of interface fracture in concrete–rock specimens on mode mixity. Eng Fract Mech 124:287–309. https://doi.org/10.1016/j.engfracmech.2014.04.030